SUPERCOLLIDER PHYSICS

Ian Hinchliffe
Lawrence Berkeley Laboratory
University of California
Berkeley, California 94720

This talk is concerned with the physics opportunities of an extremely high energy proton-proton or proton anti-proton machine. (SSC) It is based on work done in collaboration with E. Eichten, K. Lane and C. Quigg.[1] We set out to determine how the physics reach of a high energy collider is affected by its energy, luminosity and type of beam. I shall select a few topics and discuss them in this talk, the reader may refer to Ref. 1 for a more complete discussion.

The triumph of the Glashow-Weinberg-Salam model[2] in correctly predicting the W and Z masses[3] has made even more acute the problem of how the electro-weak symmetry is broken. We have almost no experimental guidence into the dynamics of this breaking. The simplest option for this dynamics is that the breaking is caused by a scalar field acquiring a vacuum expectation value. The simplest model of this type has only one physical particle, the Higgs. Unfortunately the constraints on the Higgs mass are rather weak $7\ \text{GeV} < m_H < 1\ \text{TeV}$. The lower bound comes from cosmology.[4] The upper bound is looser, it is derived from the observation[5] that a Higgs with more mass becomes strongly interacting, implying that phenomena not present in perturbation theory must occur. Many theorists regard this single Higgs possibility as unappealing.† The quadratic divergences present in perturbation theory lead to instabilities in the mass of the Higgs.[7] This is sometimes phrased in terms of a hierarchy problem which, put at its simplest, is the inability to understand why the scale of the Fermi constant ($1/\sqrt{G_F} \approx 300$ GeV) is much less than the Planck mass ($\sim 10^{19}$ GeV) or the scale of grand unification ($\sim 10^{14}$ - 10^{17} GeV) if the latter exists.

Many theoretical alternatives to this simple Higgs mechanism exist. Supersymmetric[8] models, where the Higgs is saved from these quadratic divergences by having a partner spin 1/2 particle, predict a host of new particles with the same quantum numbers as those in the standard model but with spin different by 1/2 unit. In technicolor models[9] the Higgs is not an elementary particle but is a bound state of a new fermion anti-fermion pair. The proliferation of quarks and leptons has also led to the suggestion that quarks and leptons are not elementary particles but are built from some more fundamental particles (composite models).[10] All these alternatives (except perhaps the last) have one feature in common; they all predict new physics on the scale of the Fermi-constant. It is this scale that a high energy hadron-hadron collider will probe. Since no particular model is compelling, the machine requirements can best be defined by performing some kind of ensemble average over all these models. This done in Ref. 1.; the rest of this talk

---

† The scatological significance was recently discussed by S. Glashow.[6]

is arranged as follows. I first discuss the parton model and the structure functions needed to estimate the production rates. I then discuss hadronic gets, production rates of gauge bosons, searching for the Higgs, signals for compositness, and for a sequential heavy lepton. Supersymmetric predictions and those dealing with technicolor and non-minimal Higgs are discussed by some other speakers.[11]

A) The Parton Model

Production rates in a hadron collider with center of mass energy $\sqrt{s}$ are given by

$$\sigma_H = \sum_{ij} \int dx_1 dx_2 f_i(x_1,Q^2) f_j(x_2, Q^2)\, \sigma_{ij}(\hat{s}, \hat{t}, \hat{u}) \qquad (1)$$

where $\sigma_{ij}(\hat{s}, \hat{t}, \hat{u})$ is the cross section for producing a particle of interest in a collision of two constituents of the beams labeled ij; they could be quarks or gluons. $f_i(x_1, Q^2)$ is the probability of finding a constituent of type i inside the beam particle with momentum fraction x of the beam. Q^2 is some scale characteristic of the hard scattering process (σ_{ij}) e.g. $\hat{s} = x_1 x_2 s$. The $f_i(x, Q^2)$ fall rapidly with x, so if we are interested in producing some new particle with mass M, $x_1 x_2 > M^2/s$ and most of the integral (1)is dominated by $x \sim M/\sqrt{s}$. Typically $\sigma_{ij} \propto c/\hat{s}$, with $c \sim \alpha_s^2$ for a strong interaction process such as the production of a jet pair or a heavy quark, and $c \sim \alpha_{EM}^2$ for the production of a pair of gauge bosons.

At a collider with $\sqrt{s} = 40$ TeV, we could be interested in masses as low as 100 GeV (inaccessable at LEP) or as high as 10 TeV implying

$$(100)^2\,\text{GeV}^2 < Q^2 < (10^4)^2\,\text{GeV}^2, x > 10^{-5} \qquad (2)$$

with dominant region around $x \geq 10^{-2\,1/2}$ It is straightforward in principle to obtain these distributions. One takes data at all x for some small value of Q^2 from deep inelastic scattering experiments and uses the Altarelli-Parisi equations[12] to evolve up in Q^2. The problems we encounter are as follows.

1. Data do not exist below x = 0.01, and different sets of data are not consistent with each other.
2. t and b quark distributions may be needed, and the t quark mass is unknown.
3. The gluon distribution $g(x, Q^2)$ is not directly measured, rather it is inferred from the Q^2 evolution of the anti-quarks.
4. The QCD parameter Λ is not well known and is correlated with $g(x, Q^2)$.
5. QCD perturbation theory may not be applicable at large and small values of x. The large x region is irrelevant since $f(x, Q^2)$ is very small there. The small x region is more problematic but again is not relevant for setting the upper reach of a machine (the largest M which can be produced) since for most processes this limit is set by $x \sim 0.1$ or greater.

In order to estimate the effects of these uncertainties (we can do nothing about the last one) the following technique was adopted[1]. Two parametizations based on those of the CDHS collaboration[13] were evolved and compared. These parameterizations differ in that a different value of $R = \sigma_L/\sigma_T$ was assumed in the analysis. At $Q^2 = 5\ \text{GeV}^2$ the values of $xg(x, Q^2)$ and x are

$$\text{set 1: } xg(x, Q^2) = (2.62 + 9.17x)(1-x)^{5.9}, \Lambda = .2\,\text{GeV} \qquad \text{(a)}$$

$$\text{set 2: } xg(x, Q^2) = (1.75 + 15.575x)(1-x)^{6.03}, \Lambda = .29\,\text{GeV} \qquad \text{(b)} \qquad (3)$$

As usual the gluon distribution with more support at large x (set 2) is correlated with a larger value of Λ. Figure 1 shows the behavior of $x\,g(x, Q^2)$ as a function of Q^2 for various x (set 1 shown). The difference between the two sets is less than 20% over the entire x and Q^2 range ($Q^2 < 10^8$ GeV^2).

In order to estimate the possible uncertainties associated with the absence of data in the small region, the input distributions were changed for $x < 0.01$ as follows.

$$xg(x, 5) = \begin{cases} 25.50\, x^{1/2} & \text{(a)} \\ .44\, x^{-1/2} - 1.886 & \text{(b)} \end{cases} \tag{4}$$

These match at $x = 0.01$ onto 3(a). At $Q^2 = 5$ and $x = 10^{-4}$ 4(a) and 4(b) differ by a factor of 160, but at $Q^2 = 1000$ GeV^2 the difference is order 2. These conclusions are encouraging because they suggest that the uncertainties decrease as Q^2 increases, and the differences in the starting distributions wash out. (See also Ref. 14.) Comparisons with other deep inelastic scattering data e.g. those of the CHARM collaboration[15] indicate that our anti-quark distributions may be too small (Fig. 2). These problems cannot be resolved until the data in the same Q^2 region agree. The effect of a change in Λ from .2 GeV to .1 GeV for 3(a) is less than 30% over the entire range of x and Q^2.

A useful quantity to estimate the reach of a collider is

$$\tau/\hat{s}\, d\mathcal{L}/d\tau \equiv \tau/(1+\delta_{ij}) \int (f_i(x, Q^2)\, f_j(\tau/x, Q^2) + i \leftrightarrows j) dx/xs \tag{5}$$

This quantity has the dimension of a cross-section and can be used to estimate the production rate of strongly interacting objects by multiplying by α_s^2. Figure 3 shows this quantity as a function of s at fixed s for gluon gluon collisions in pp collisions. (The $p\bar{p}$ rate is the same.) It can be seen from this figure that at $\sqrt{s} = 40$ TeV there will be a reasonable number of events at $\sqrt{\hat{s}} \sim 10$ TeV for a strong interaction process at a luminosity of 10^{33} cm^{-2}sec^{-1}. The figure shows the price paid in the reach of a machine at fixed energy as the luminosity is lowered. The same number of events at $\mathcal{L} = 10^{31}$ cm^{-2}sec^{-1} is reached at $\sqrt{s} \approx 3$ TeV.

Figure 4 shows $\tau/\hat{s} d\mathcal{L}/d\tau$ for $u\tilde{u}$ collisions in pp colliders. The ratio $p\bar{p}/pp$ is shown in Figure 5. These two figures show that a certain minimum luminosity is required to exploit the advantage of pp. For a weak process (e.g.the cross section $d\sigma/dp_t dy$ for the p_t the production of a heavy gauge boson) the rate is roughly $\alpha_{EM}\, \tau d\mathcal{L}/d\tau/s$. If we take a year of 10^7 seconds and require 1000 events Fig. 4 shows that a $\sqrt{s} = 40$ TeV machine reaches $\sqrt{\hat{s}} \sim 7, 4, 2$ TeV at luminosities of 10^{32}, 10^{32}. 10^{31} cm^{-2} sec^{-1}. Figure 5 now shows that at the smallest of these luminosities there is essentially no advantage in a pp machine. As σ_{ij} decreases the advantage of pp at the same luminosity becomes weaker.

B) Hadronic Jets

Hadronic jets at large transverse momenta (p_t) will present a background to new physics at a high energy collider so it is important that they be well understood. Given parton distributions there are still uncertainties in the production rate. The scale Q^2 which appears $\alpha_s^2(Q^2)$ controlling the $2 \to 2$ scattering process and appears in $f(x, Q^2)$ is undetermined. We use $p_T^2/4$ (see Ref. 14 and 16), this uncertainty is more

important at the Sp$\bar{p}$S collider than at higher energies. Figure 6 shows the cross section $d\hat{\sigma}/dp_t dy$ at $y = 0$ for the Sp$\bar{p}$S collider. A comparison with the data[17] reveals no gross differences. The contributions of the different final states, gluon-gluon, gluon quark and quark quark are shown separately. Notice that configurations with gluons in the final state dominate over the region of most of the data. The cross section at $\sqrt{s} = 40$ TeV is shown in Fig. 7 and at $\sqrt{s} = 10$ TeV in Fig. 8. Even a high luminosity machine will have great difficultly in obtaining a clear sample of quark jets. The production rate of these jets is enormous; Fig. 9 shows the cross section for the production of two jets with rapidity y constrained, $|y| < 2.5$ and transverse energy E_T greater than E_{T_0} for $\sqrt{s} = 10, 40, 100$ TeV as a function of E_{T_0}. At a luminosity of 10^{33} cm^{-2} sec^{-1} the rate of jet production for $E_{T_0} = 1$ TeV at $\sqrt{s} = 40$ TeV is 400 Hz. The production rate in pp and p$\bar{p}$ colliders at the same $\sqrt{s}$ is equal to within 20%. The number of three jet events is also impressively large.[1]

C) Production of Gauge Bosons.

The total cross sections for the production of W^+ in pp and p$\bar{p}$ collisions is shown in Fig. 10. Since $\hat{s} = M_W{}^2$ and hence τ is rather small at $\sqrt{s} = 40$ TeV the production rate is dominated by sea quarks and the advantage in rate provided by the valence anti-quarks in p$\bar{p}$ collisions is extremely slight. At $\sqrt{s} = 40$ TeV the production rate is very large ($\sim$ 120 nb) but most of the W's are produced at small angle. Figure 11 shows the rapidity distribution; approximately 75% of the W's are emitted within 5^0 of the beam.

There may exist new W's with a larger mass than 100 GeV. If we assume a coupling to quarks equal to that of the standard W the production rate of Fig. 12 is obtained. The cross-section has been integrated requiring that the new W has $|y| < 1.5$ and the figure shows pp collisions. The rate for p$\bar{p}$ is lightly larger (Fig. 13) but again a minimum luminosity is needed to exploit the advantage. If we require 1000 produced new W's, which should be enough to discover one, given a reasonable branching ratio into $\nu\ell$, we obtain a maximum mass which can be explored at fixed values of $\sqrt{s}$ and integrated luminosity. Figure 14 shows this mass as a function of $\sqrt{s}$ for different values of $\int$£dt in a pp machine. It can be seen that a 10^{33}cm^{-2}sec^{-1} machine at $\sqrt{s}$ of 40 TeV can reach masses of 7 TeV.

D) Searching for the minimal Higgs

The Higgs is not a typical member of the zoo of particles predicted by models to have masses in the 1 TeV region. It has a rather small production cross-section and is one of the most difficult particles to see. In this respect it places the strongest demands upon energy and luminosity. If the Higgs is lighter than 2 M_W, it decays into heavy quarks ($t\bar{t}$ if $m_H > 2m_t$, $b\bar{b}$ otherwise). In this case the background is from the QCD production of heavy quarks, assuming that the detector can distinguish between light and heavy quarks. This background is much greater than the signal,[1] so it seems difficult to detect a light Higgs unless its production rate is much larger than the estimate given here.† If $m_H > 2M_W$ or $2M_Z$, it decays almost exclusively into ZZ and WW final states with a width

† A larger rate may be possible in non-minimal models with more than one physical Higgs particle.

$$\Gamma(H \rightarrow WW) = 2\Gamma(H \rightarrow ZZ) = 320\, m_H^3\ GeV \qquad (6)$$

where m_H is measured in TeV. Two mechanisms for the production of the Higgs are relevant. Gluon-gluon fusion[18] via an intermediate quark loop yields the rate shown in Fig. 15. The rate is sensitive to the top quark mass, and also to the presence, if any, of extra generations. $M_t = 30$ GeV has been used and the figure should probably be viewed a lower bound on the production rate for this mechanism. The Higgs can also be produced by WW (or ZZ) fusion.[19] The rate for this process is shown in Fig. 16. At large values of m_H this mechanism dominates since it exploits the large width for $H \rightarrow WW$.

The signal for a heavy Higgs will be a peak in the invariant mass of a W or Z pair.[20] The background is from the continuum production of W pairs.[21] Figure 17 shows the cross-section for $pp \rightarrow W^+W^- + X$ as a function of energy. The W's from the continuum are produced with a flatter rapidity distribution than those from Higgs decay. Fig. 17 also show the rate if the W's are restricted to have rapidity less than 2.5 or 1.5. Figure 18 shows the signal and background in the W pair channel for a Higgs produced at $\sqrt{s} = 40$ TeV. The W's are required to have rapidity less than 2.5. The background is obtained from $\Gamma_H\, d\sigma/dM$ where M is the mass of a pair of W's produced in the continuum. The signal and background are comparable. Figure 19 shows the signal and background at $\sqrt{s} = 10$ TeV. The signal to noise ratio is worse.

Luminosity is extremely critical, as is the efficiency with which the W's (or Z's) can be detected. It may be possible to detect W pairs from the hadronic modes of the W. There is a large background from the QCD production of multi jets and a preliminary study of the problem[22] indicates that this will be very difficult. If gauge bosons can only be detected in leptonic modes, only the ZZ final state can probably be clearly reconstructed with an efficiency of $(0.06)^2$. Figure 20 shows the signal and background in this channel. For $m_H = 500$ GeV there are approximately 10 detected events for $\int £dt = 10^{40}$, which is probably enough given the cleanliness of the signal. One will have to look hard to find a Higgs but it does seem possible. The production rates in $p\bar{p}$ are the same but the background is somewhat worse.[1] One final word; the production rates used could be too small if the t quark mass is larger than 30 GeV or if there are more generations of quarks.

E) The search for compositness of quarks and leptons.

The proliferation of quarks and leptons has led to speculation that they may not be pointlike particles but are rather built from some more fundamental objects called preons. These preons are bound together by a new force with a binding scale Λ. At energies much less than Λ, this composite structure could manifest itself as a four fermion interaction between quarks of the following form.[23]

$$g^2/\Lambda^2\, \bar{\psi} A \psi \bar{\psi} B \psi \qquad (7)$$

Here ψ represents a quark, g is the coupling strength of the new interaction whose spin structure is specified by A and B. This term is a low energy residue of the new interaction and will interfere with one gluon exchange to produce a cross-section for quark quark scattering at wide angle and center of mass energy $\sqrt{s}$, which has the following symbolic form

$$\sigma \sim E\, a_s^2/s + F\, a_s g^2/\Lambda^2 + G\, s g^4/\Lambda^4 \qquad (8)$$

Here E, F, G depend on the scattering angle and F and G also depend on the detailed structure specified by A and B. This form is valid only when $s < \Lambda$.[2]

If we assume that the interaction (7) is diagonal in flavor and that the coupling involves only left handed quarks ($A, B \sim \gamma^{\mu}(1 - \gamma_5)$)), then we obtain the result shown in Fig. 21 which shows the effect on the jet cross-section $d^2\sigma/dp_T dy$ at $y = 0$ and $\sqrt{s} = 40$ TeV in pp collisions as a function of Λ for $g^2/4\pi = 1$. The scale Q^2 in the parton distributions was taken to be P_T^2, a comparison with Fig. 7. reveals the sensitivity to this choice (see section B). For the values of Λ shown the effects of the second and third terms in equation 8 are comparable.

A search for substructure involves looking at the jet cross-section and seeing that it is flatter in p_T than expected from QCD alone. There is a potential problem in that the QCD expectation depends on the structure functions which need to be known with reasonable accuracy. Fortunately, regions of x relevant are such that one can have confidence that the structure function uncertainties are less than a factor of two. The following criterion should be adequate for detecting a composite effect. If $\Delta(p_T)$ is greater than one or less than 0.5 where

$$\Delta(p_T) \equiv \frac{d^2\sigma/dp_T dy|_{observed} - d^2\sigma/dp_T dy|_{QCD}}{d^2\sigma/dp_T dy_{observed}} \qquad (9)$$

If we ask that this criteria be satisfied and that there be more than 50 events per unit of y then the 40 TeV collider has sensitivitity up to $\Lambda = 15$ TeV for an integrated luminosity of 10^{40} cm^{-2} sec^{-1}.

F) Searching for a heavy lepton

One is used to thinking that it is very difficult to find a heavy lepton in a hadron collider since the production rates are small and the signal poor. However, a new heavy lepton L appearing in a doublet (L, N) will decay $L \rightarrow W + N$ if $m_L - m_N > m_W$. I will assume that the mass of the new neutrino N is very small. L^+L^- can be produced in pairs in the Drell-Yan mechanism. The final state will consist of W^+W^- + missing momentum (carried off by N) giving a signature which should be recognizable even with the small rate.

The lepton can also be produced singly by the weak analog of the Drell-Yan mechanism

$$q\bar{q} \rightarrow W^* \rightarrow LN \qquad (10)$$

this process leads to a single W in the final state at large p_T with a large amount of missing p_T. Figure 22 shows $d\sigma/dy$ at $y = 0$ for the process $pp \rightarrow L^{\pm} N + X$, where y is the rapidity of the LN pair, as a function of m_L. The rates are small but the only background from old physics is the final state W + Z where the Z decays into neutrino pairs. We can estimate the background as follows. Compare the signal with $|y| < 1.5$ with the background where both W and Z have $|y| < 2.5$. This larger bin is needed to take account of the mobility of the W from L decay. Requiring an excess of 50 events of signal over background gives Fig. 23 which shows the center of mass energy needed to reach a particular lepton mass for fixed values of effective luminosity. The true luminosity is the effective value divided by the efficiency for detecting a W. If this

efficiency is 0(1/10) then at $\sqrt{s}$ = 40 TeV a collider with luminosity of 10^{33} cm^{-2} sec^{-1} can reach masses of order 700 GeV.

G) Conclusion

I will summarize very briefly the conclusions drawn from Ref. 1. Several unsolved problems concerning backgrounds prevent one from claiming that some particular signal is clearly observable. One of the most critical issues concerns the observability of W's and Z's from their decays into hadronic jets. Many signals for new physics involve final states with W's or Z's (e.g. the minimal Higgs discussed in D). If one is restricted to observing the W's and Z's via their leptonic modes (which may not be possible for final states involving more than one W) only a small number of events will be detected – 5000 Z pairs decaying into ee and μμ results in only 18 detected events. The physics background to hadronic decays of W and Z is from QCD events with multiple jets. In the case of final states with 4 jets we have no reliable QCD estimate. Many particle searches (e.g. supersymmetric ones) involve signals which have missing transverse momentum, so the importance of hermetic detectors with 4π coverage cannot be overstated.

The difference between a pp and a $p\bar{p}$ collider is limited to a few special cases where the presence of valence antiquarks in the anti-proton is important (for example in the production of a new W). In order to exploit this advantage a certain minimum luminosity is required. ($\sim 5 \times 10^{31}$ cm^{-2} sec^{-1} for $\sqrt{s}$ = 40 TeV).

In conclusion a 40 TeV machine operating at a luminosity of at least 10^{32} cm^{-2} sec^{-1}, seems capable of answering the fundamental questions surrounding the breaking of weak interactions. The same assurance cannot be given for a 10 TeV Machine at the same luminosity.

Acknowledgments

I wish to thank my collaborators Estia Eichten, Ken Lane and Chris Quigg for their unceasing efforts in our seemingly endless collaboration. The work was supported by the Director, Office of Energy Research, Office of High Energy and Nuclear Physics, Division of High Energy Physics of the U.S. Department of Energy under Contract DE-AC03-7600098.

Referances

1. E. Eichten, I. Hinchliffe, K. Lane, C. Quigg, FNAL 84/17-T, LBL-16875, DOE/ER/01545-345 (1984).
2. S. L. Glashow, *Nucl. Phys. 22, 579 (1961);*
   A. Salam in "Elementary Particle Theory" p 367 ed W. Svartholm, Almquist and Wiksell (1968).
   S. Weinberg, *Phys. Rev. Lett. 19, 1264 (1967).*
3. G. Arnison, et al., *Phys. Lett. 122B, 103 (1983); Phy. Lett. 126B, 398 (1983).*
   M. Banner, et al., *Phys. Lett. 122B, 476 (1983);*
   P. Bagnaia, et al., *Phy. Lett. 129B, 130 (1983).*
4. A. P. Linde, *Sov. Phys. JETP Lett. 23 64 (1976);*
   S. Weinberg, *Phys. Rev. Lett. 36, 294 (1976).*
5. B. W. Lee, C. Quigg, H. B. Thacker, *Phys. Rev. D16, 1519 (1977).*
6. S. L. Glashow in Science 84 February 1984.
7. K. A. Wilson, *Phys. Rev. D3, 1818 (1971).*
8. H. Haber and G. L. Kane, Phys. Rep. to appear and Refs. therein.
   S. Dawson, E. Eichten, C. Quigg, FNAL 83/82-THY (1984).
9. E. Farhi and R. Jackiw (editors) Dynamical gauge symmetry breaking. World Scientific Publishing Singapore (1982) and Refs. therein.
10. R. Peccei, these proceedings.
11. D. V. Nanopoulos, these proceeding;
    D. Wyler, these proceedings.
12. G. Altarelli and G. Parisi, *Pucl. Phys. B126, 298 (1977).*
13. H. Abramowicz et al., *Z. Physik C17, 199 (1983); C132, 83 (1982).*
14. R. K. Ellis these proceedings.
15. F. Bergsma et al., *Phys. Lett. 123B, 269 (1983).*
16. R. K. Ellis et al., *Nucl Phys. B173, 397 (1980);*
    W. Slominski, Jagellonian University Thesis (1981).
17. P. Bagnaia et al., *Z. Physik C20, 117 (1983);* CERN-EP 84/12.
18. H. Georgi, et al., *Phys. Rev. Lett. 40, 692 (1978).*
19. R. N. Cahn and S. Dawson, *Phys. Lett. 136B, 196 (1984).*
20. H. Gordon, et al., in Proceedings of the 1982 DPF Summer Study on Elementary Particle Physics and Future Facilities ed. R. Donaldson, R. Gustafson and F. Paige Batavia, IL (1982).
21. R. W. Brown and K. O. Mikaelian, *Phys. Rev. D19, 922 (1979).*
22. M. K. Gaillard, *UCB-PTH-84/2 (1984).*
    M. Shochet in Proc. of DPF study on pp colliders U. Chicago, Feb. 1974.
23. E. Eichten, K. Lane, M. Peskin, *Phys. Rev. Lett. 50, 811 (1983).*

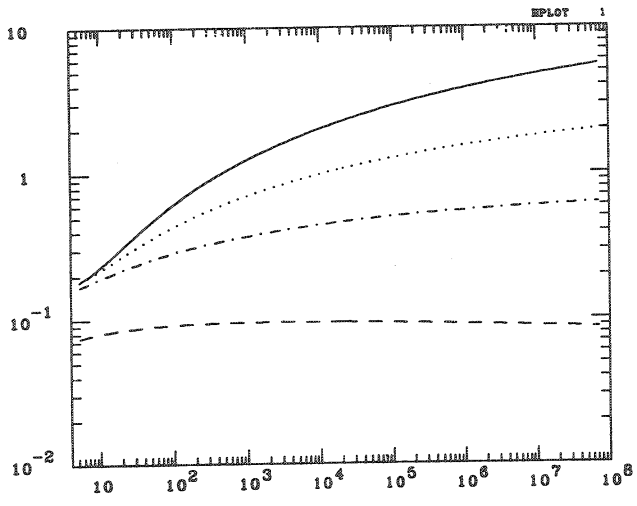

Fig. 1 The distribution $xg(x, Q^2)$ vs Q^2 in GeV^2 at $x = 10^{-4}$ (solid line) $x = 10^{-3}$ (dotted) $x = 10^{-2}$ (dot-dashed) $x = .1$ (dashed).

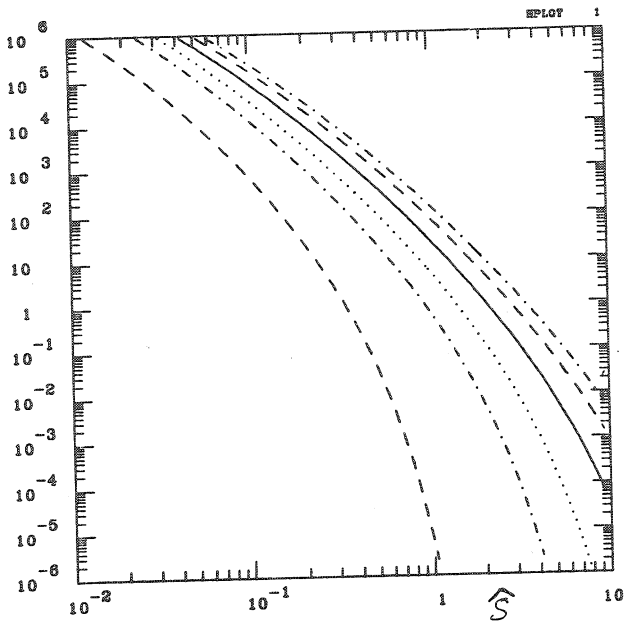

Fig. 3. The function $\tau/\hat{s}\ d\mathcal{L}/d\tau$ in nanobarns (eq. 5) as a function of $\sqrt{\hat{s}}$ for $\sqrt{s}$ = 2, 10, 20, 40, 70, 100 TeV for gluon gluon collisions.

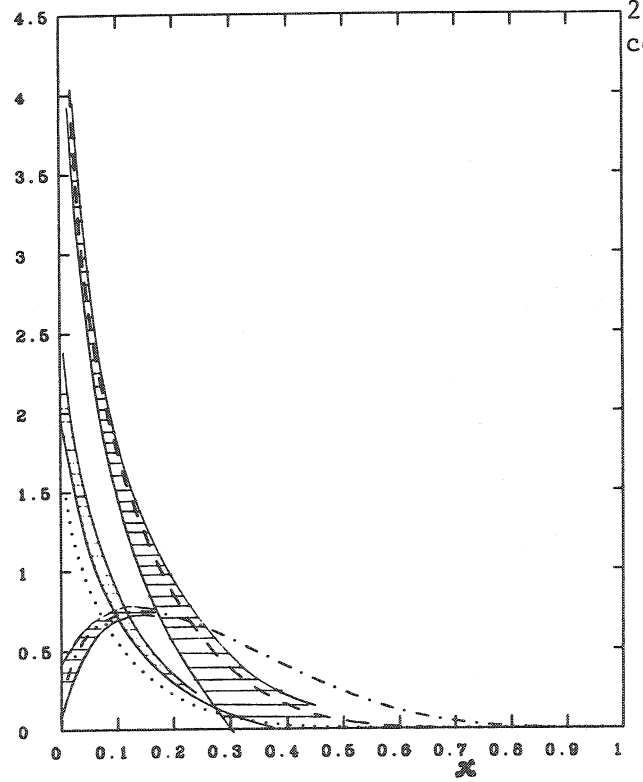

Fig. 2. Comparison at $Q^2 = 50\ GeV^2$ of x times the distribution functions, of the CHARM collaboration[15] (dashed regions) with these of Ref. 1. (dashed line) twice the anti-quarks (dotted line) and the sum of up and down valence quarks (dot-dashed line).

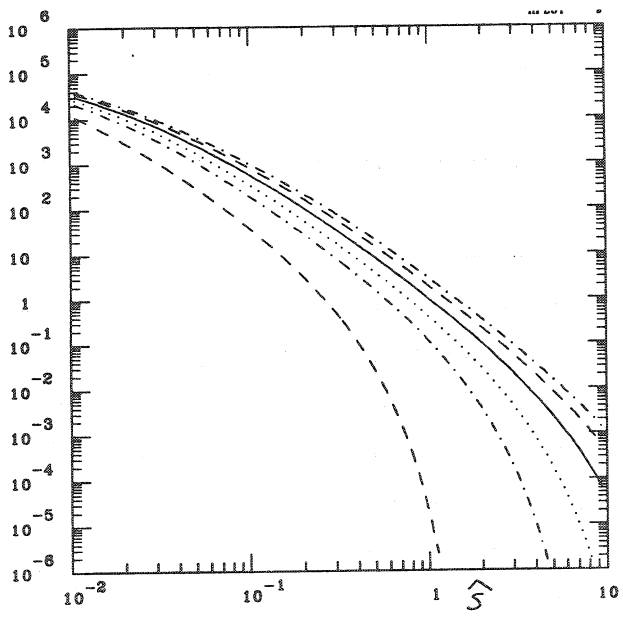

Fig. 4. The function $\tau/\hat{s}\ d\mathcal{L}/d\tau$ in nanobarn (eq. 5) as a function of $\sqrt{\hat{s}}$ for $\sqrt{s}$ = 2, 10, 40, 20, 70, 100 TeV for $u\bar{u}$ collisions in a pp collider.

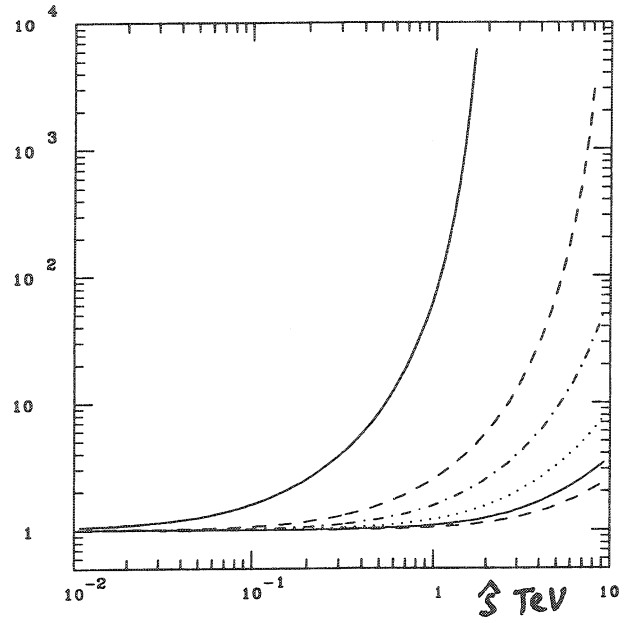

Fig. 5 The ratio of $\tau/\hat{s}\ d\mathcal{L}/d\tau$ for $u\bar{u}$ collision in $p\bar{p}$ to that in pp at $\sqrt{s}$ = 2, 10, 20, 40, 70, 100 TeV as a function of $\sqrt{\hat{s}}$.

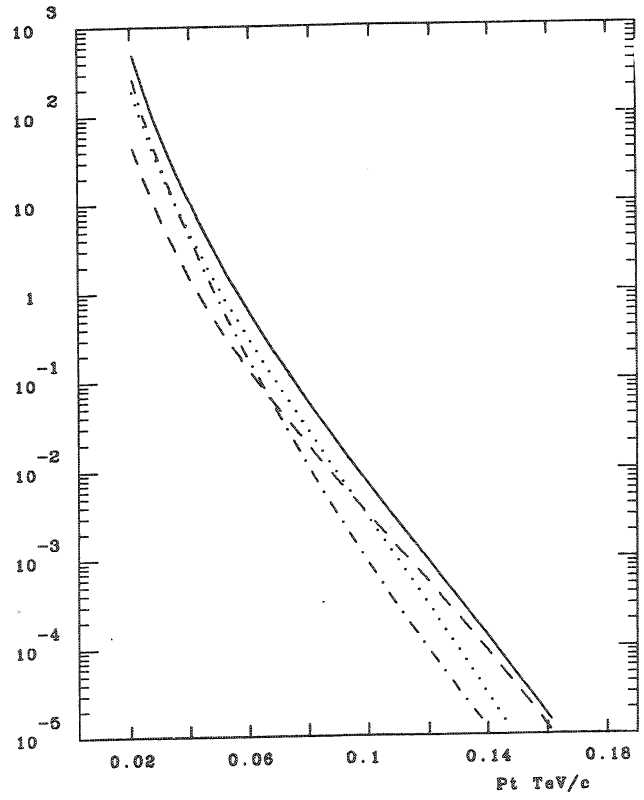

Fig. 6. The cross-section $d^2\sigma/dp_t dy$ in nb/GeV at y = 0 for the production of a jet in $p\bar{p}$ collisions at $\sqrt{s}$ = 540 GeV (solid line) the final states, gluon gluon (dot dashed) gluon quark (dotted) and quark quark (dashed) are shown separately.

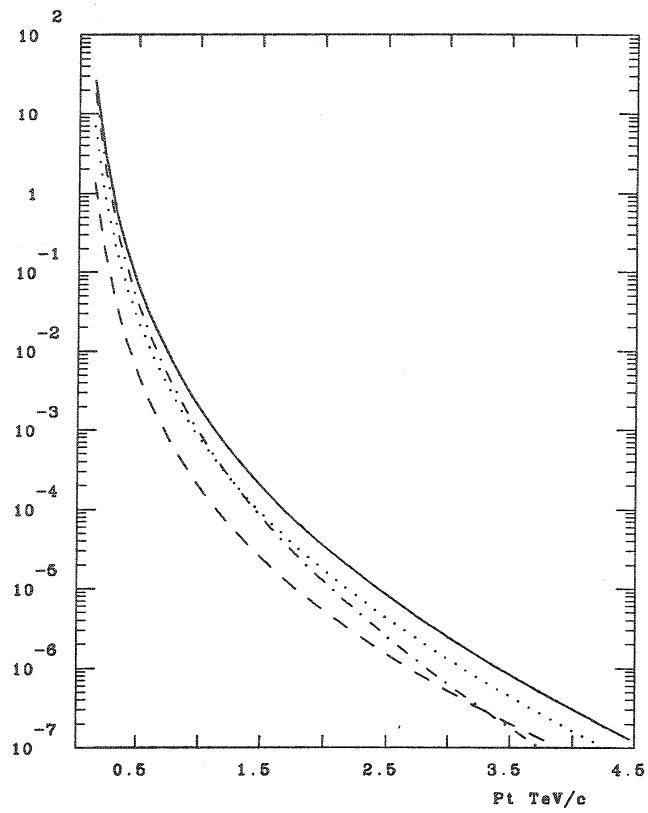

Fig. 7. As Fig. 6 except for pp collisions at $\sqrt{s}$ = 40 TeV.

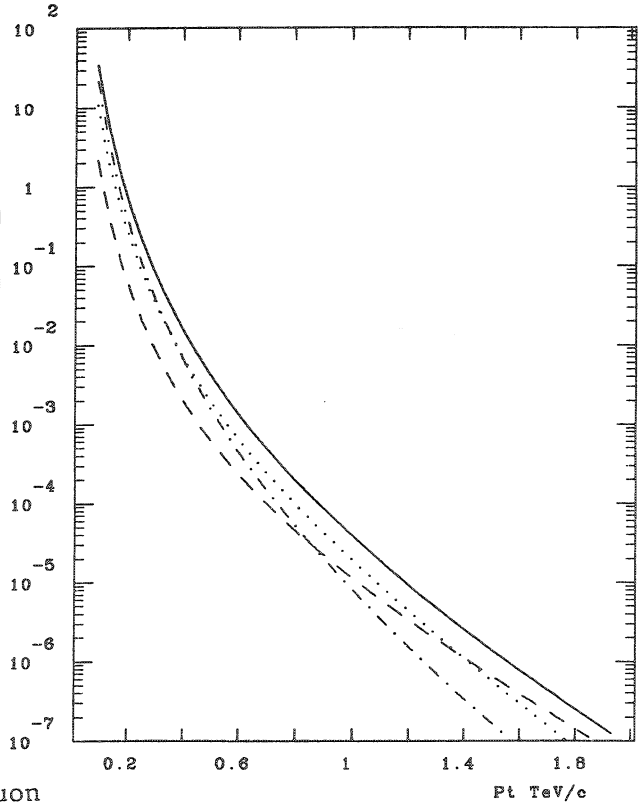

Fig. 8. As Fig. 6 except for pp collisions at $\sqrt{s}$ = 10 TeV.

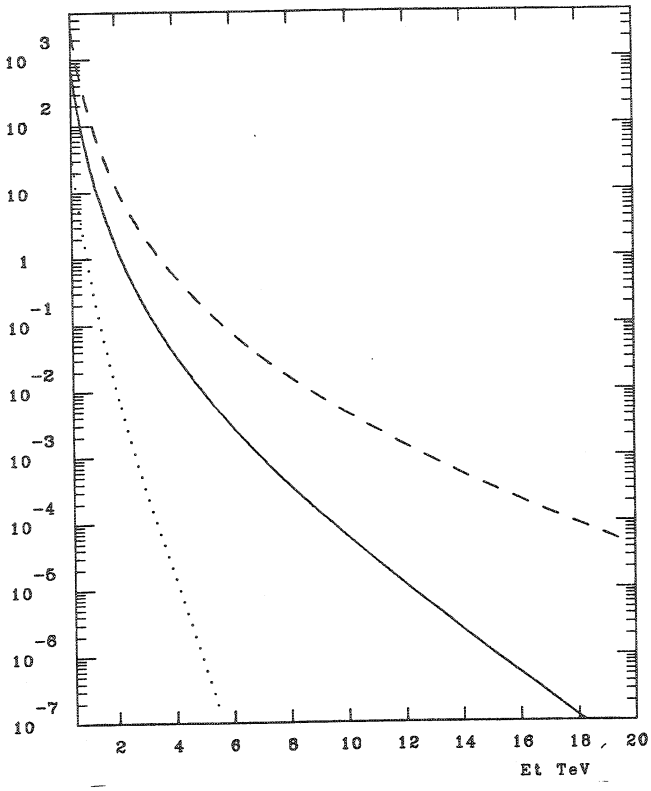

Fig. 9. The cross-section in nanobarns for the production of a pair of jets each with $|y| < 2.5$ and with total transverse energy greater than E_{T0}. $\sqrt{s}$ = 10, 40, 100, TeV shown.

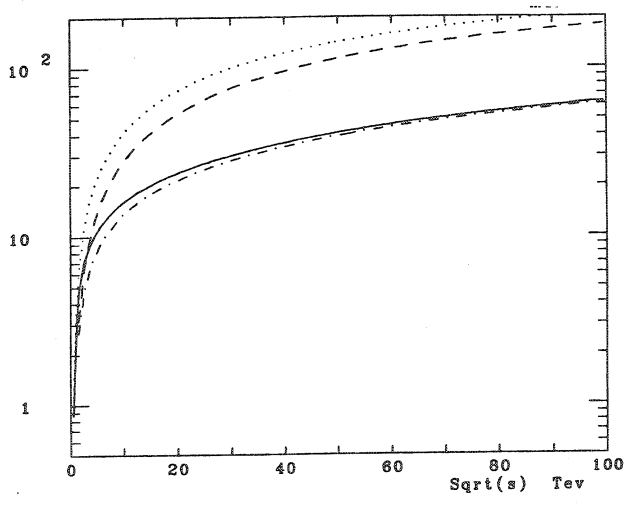

Fig. 10 The total cross section in nanobarns for the production of W^+ (dotted line), W^- (dashed line) in pp collisions as a function of $\sqrt{s}$. Also shown are the rates $|y_W| < 1.5$.

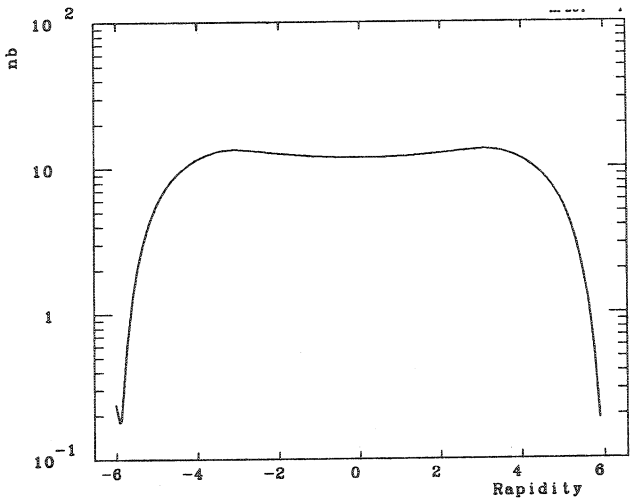

Fig. 11 The rapidity distribution $d\sigma/dy$ in nanobarns for the production of W^+ in pp collisions at $\sqrt{s}$ = 40 TeV.

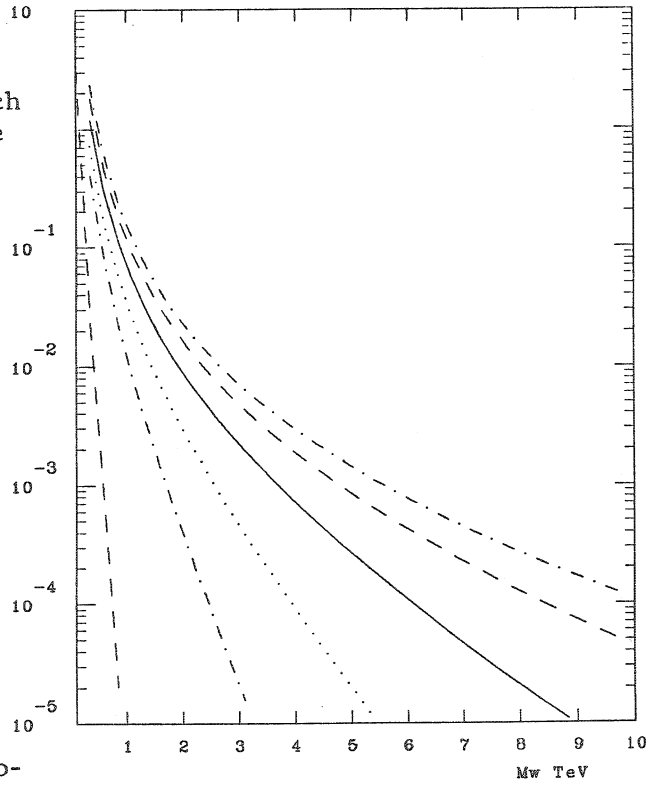

Fig. 12. The cross section for pp → $W^{+\prime}$ in nanobarns as a function of the mass of the new $W^{+\prime}$. The $W^{+\prime}$ is contrained to have $|y| < 1.5$. $\sqrt{s}$ = 2, 10, 20, 40, 70, 100 TeV shown.

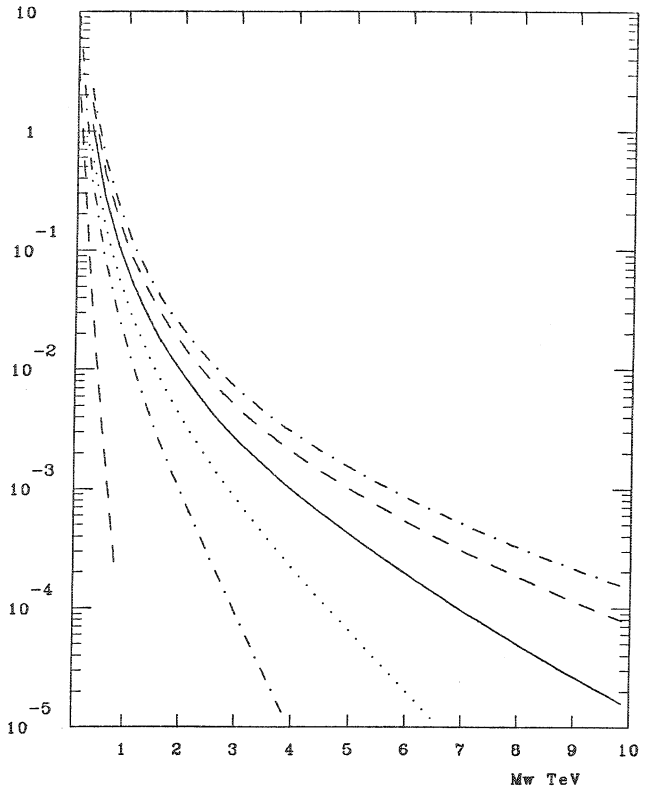

Fig. 13. As in Fig. 12 except for $p\bar{p}$ collisions.

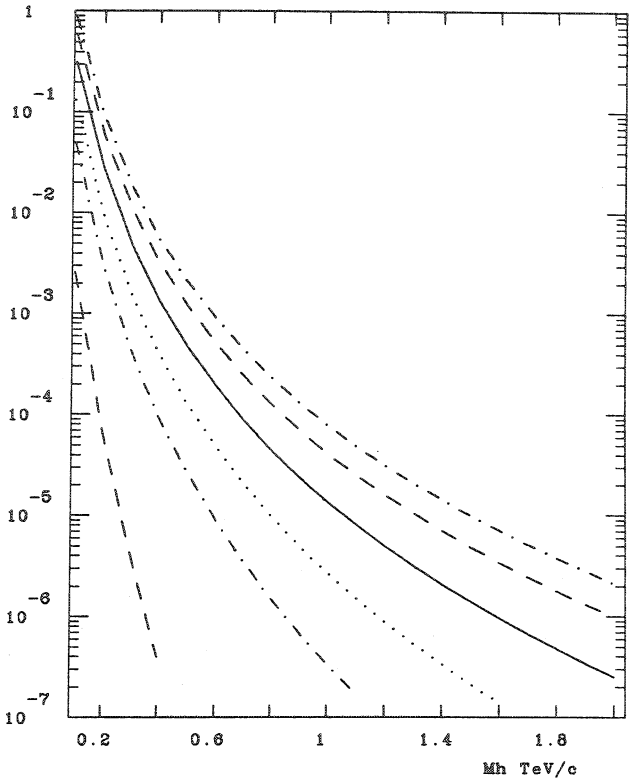

Fig. 15. Higgs production cross-section in nanobarns from gluon fusion mechanism[18] as function of m_H. $\sqrt{s}$ = 2, 10, 20, 40, 70, 100 TeV shown.

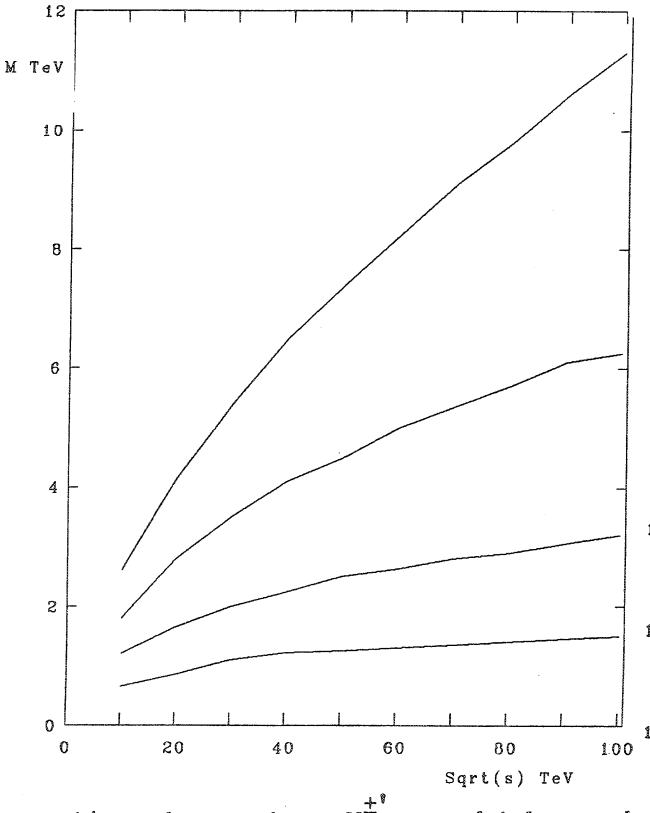

Fig. 14. The maximum $W^{\pm}$ mass which can be reached as a function of $\sqrt{s}$ for integrated luminosities of 10^{37}, 10^{38}, 10^{39}, 10^{40} cm^{-2}. (pp collisions)

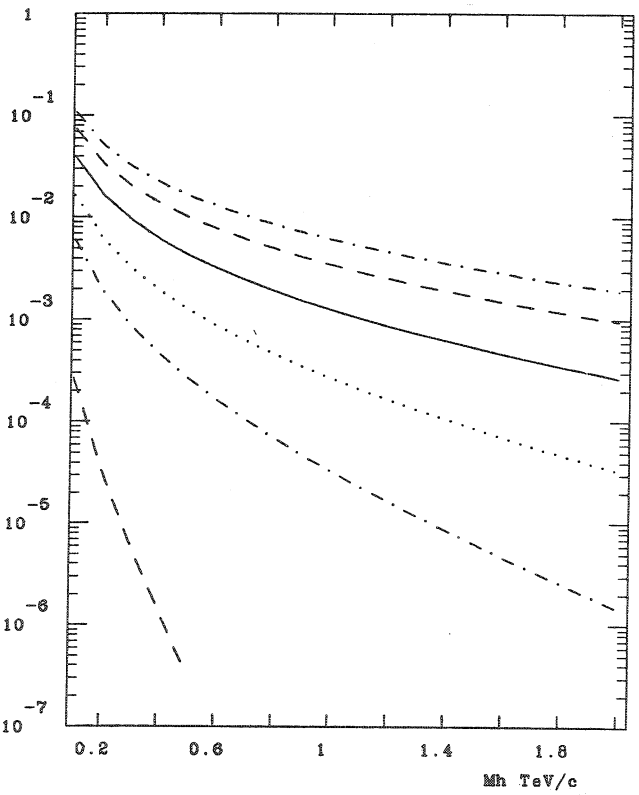

Fig. 16. Higgs production cross section in nanobarns via the gauge boson fusion mechanism[19]. A function of m_H. $\sqrt{s}$ = 2, 10, 20, 40, 70, 100 TeV shown.

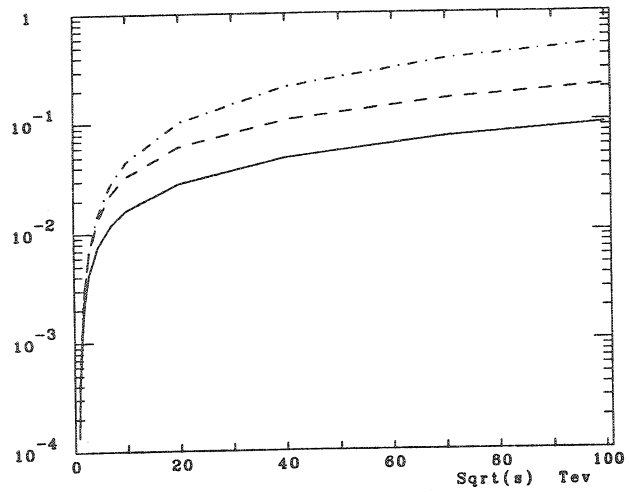

Fig. 17. Cross section in nanobarns for $pp \to W^{\pm}W^{-} + X$ as a function of $\sqrt{s}$. The lines are the total cross section and the cross-section contrained by $|y_W| < 1.5$ and $|y_W| < 2.5$.

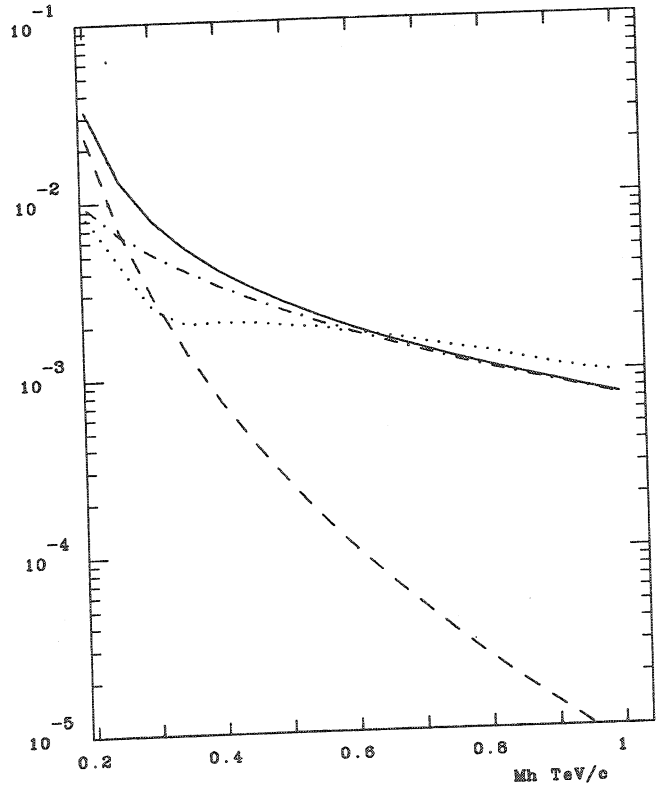

Fig. 18. Signal and background in nanobarns for the process $pp \to H \to W^{\pm}W^{-}$ with $|y_W| < 2.5$ at $\sqrt{s}$ = 40 TeV.

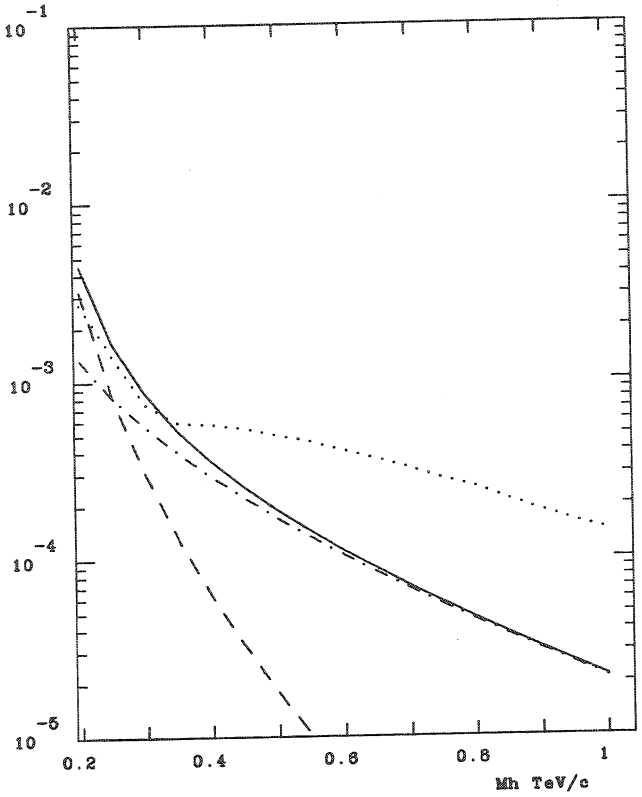

Fig. 19. As Fig. 18 except $\sqrt{s}$ = 10 TeV.

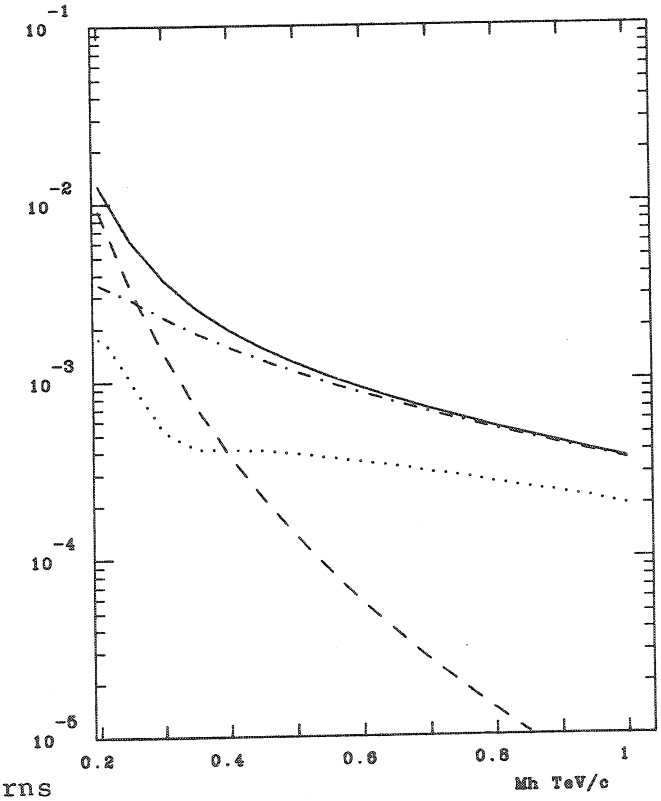

Fig. 20. Signal and background in nanobar for the process $pp \to H \to ZZ$ with $|y_z| < 2.$ at $\sqrt{s}$ = 40 TeV.

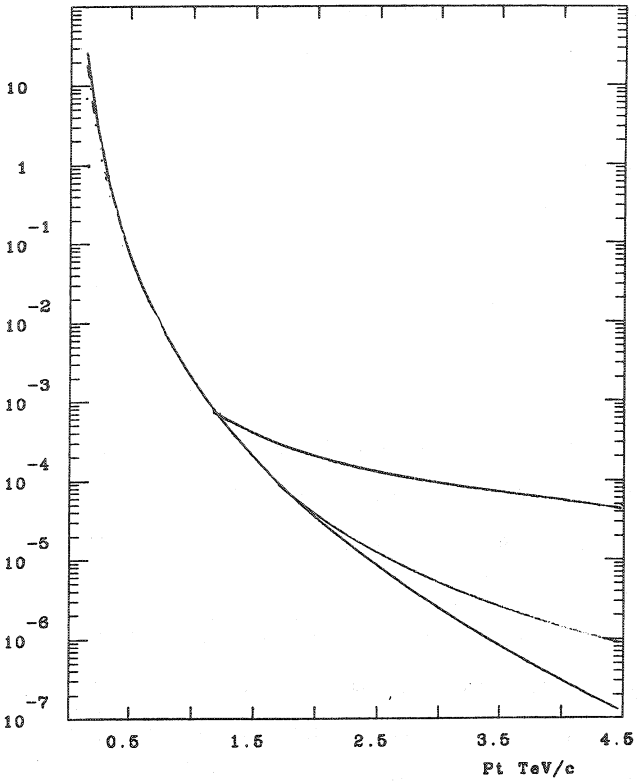

Fig. 21. The jet cross section $d\sigma^2/dp_t dy$ at $\sqrt{s}$ = 40 TeV and y = 0 in nanobarns/GeV as a function of p_t showing the effect of the term Eq. 8. Λ = 5, 10, 20 TeV shown.

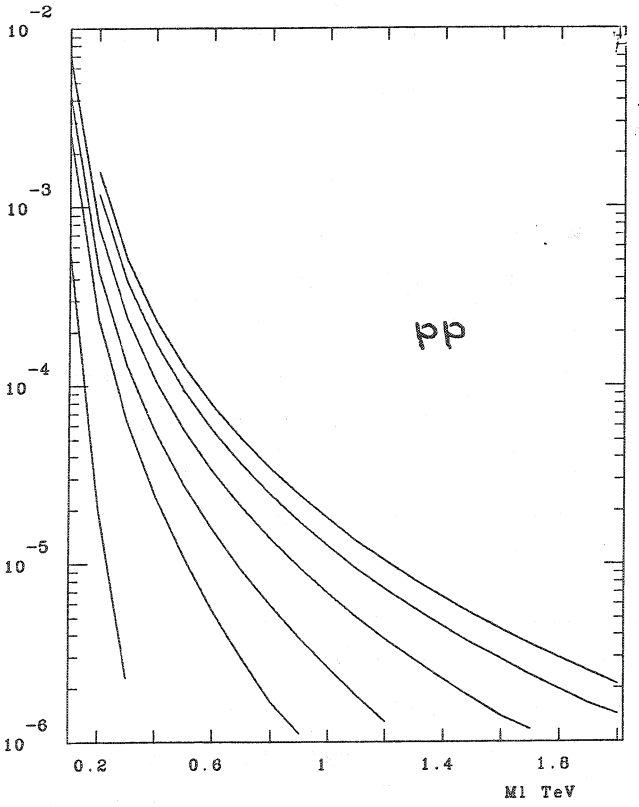

Fig. 22. The cross section $d\sigma/dy$ in nanobarns at y = 0 for the production of an (LN) pair by the process of Eq. 10. $\sqrt{s}$ = 2, 10, 20, 40, 70, 100 TeV

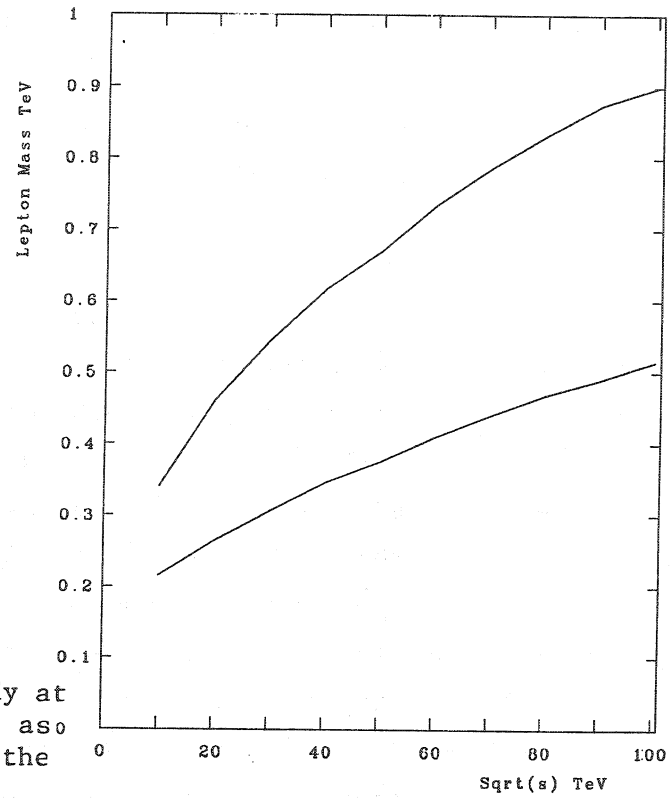

Fig. 23. Maximum mass for L which can be reached as a function of $\sqrt{s}$ for effective int. luminosities of 10^{37}, 10^{38} cm^{-2} according to the criteria of Section F.